Potential of curcumin-loaded cubosomes for topical treatment of cervical cancer

Francesca Damiani Victorelli [a,b], Livia Salvati Manni [a], Stefania Biffi [c], Barbara Bortot [c], Hilde Harb Buzzá [d,e], Viviane Lutz-Bueno [a,j], Stephan Handschin [a], Giovana Calixto [f], Sergio Murgia [g,h], Marlus Chorilli [b], Raffaele Mezzenga [a,i,*]

[a] Department of Health Sciences and Technology, ETH Zurich, 8092 Zurich, Switzerland
[b] Department of Drugs and Medicines, School of Pharmaceutical Sciences, São Paulo State University, 14800-903 Araraquara, Sao Paulo, Brazil
[c] Institute for Maternal and Child Health-IRCCS "Burlo Garofolo", Trieste, Italy
[d] São Carlos Institute of Physics, University of São Paulo (USP), 13560-970 São Carlos, São Paulo, Brazil
[e] Institute of Physics, Pontificia Universidad Católica de Chile, Santiago 7820436, Chile
[f] UNICAMP, University of Campinas, Piracicaba Dental School, Department of Biosciences, Piracicaba, São Paulo 13414-903, Brazil
[g] Department of Life and Environmental Sciences, University of Cagliari, 09042 Monserrato, Cagliari, Italy
[h] CSGI, Consorzio Interuniversitario per lo Sviluppo dei Sistemi a Grande Interfase, via della Lastruccia 3, 50019 Sesto Fiorentino, Florence, Italy
[i] Department of Materials, ETH Zurich, 8093 Zurich, Switzerland
[j] Paul Scherrer Insiture PSI, 5232 Villigen, Switzerland

GRAPHICAL ABSTRACT
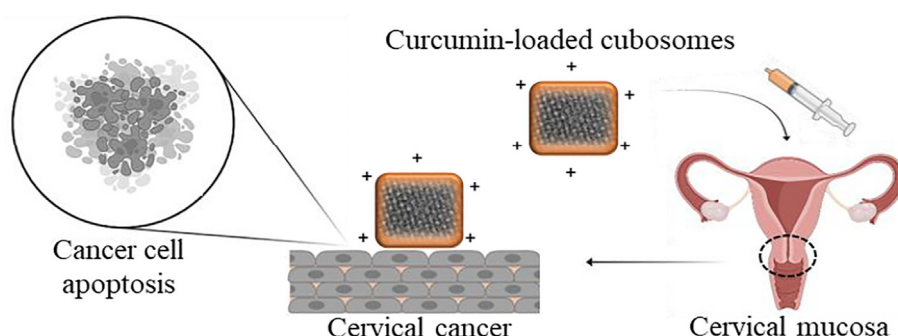
ARTICLE INFO

ABSTRACT

Cervical cancer is one of the most common cancers affecting women worldwide. There are an estimated 570.000 new cases of cervical cancer each year and conventional treatments can cause severe side effects. In this work, we developed a platform for vaginal administration of lipophilic drugs for cervical cancer treatment. We formulated mucoadhesive cubosomes for the delivery of curcumin, a lipophilic drug for cervical cancer treatment, to increase its bioavailability and local absorption. This study tests the use of cubosomes for vaginal drug administration and assesses their potential efficiency using the CAM (chick embryo chorioallantoic membrane) model. SAXS (small-angle X-ray scattering), cryo-TEM (cryo-transmission electron microscopy), and dynamic light scattering (DLS) were employed to characterise the system. With *ex vivo* permeation and retention studies, we find that the curcumin released from

our system is retained in the vaginal mucosa. *In vitro* cytotoxicity assay and cellular uptake showed an increased cytotoxic effect of curcumin against HeLa cell line when incorporated into the cubosomes. The curcumin-loaded cubosomes also demonstrated an antiangiogenic effect evaluated *in vivo* by the CAM model.

1. Introduction

Cervical cancer is one of the most common cancers that affect women globally [1–3]. The conventional treatments are surgery, radiotherapy, or radiochemotherapy. In addition to being expensive, these treatments negatively impact the quality of women's lives by causing several side effects, such as hair loss, immunosuppression and nausea, and often have an unfavourable prognosis [3]. One current strategy to reduce the side effects of treatments is to explore less invasive drug delivery routes.

Interest in the vaginal drug delivery route has increased markedly in recent years, because it is non-invasive, and serves as an alternative administration route for drugs that are poorly absorbed orally [4–7]. The human cervicovaginal surface presents a dense network of blood vessels that makes it an excellent route of drug delivery for both systemic and local effect. Among other advantages are the ability to bypass first pass metabolism, the reduction in the incidence and severity of gastrointestinal and/or hepatic side effects, ease of administration, high permeability for many active ingredients, high drug levels at the target site, minimization of side effects associated with systemic therapy, and self-administration at longer intervals [7–9]. Extant literature reports that curcumin-loaded microemulsion for vaginal administration can be employed as efficient antifungal against *Candida albicans* [10], and that PLGA (poly (D,L-lactide-*co*-glycolide)) nanoparticles with chitosan are efficient vaginal delivery systems for antimycotic drugs [11]. Moreover, PEGylated liposomes with siRNA (small interfering RNA) can be employed as a vaginal delivery system for gene therapy [12].

Curcumin is a natural product isolated from rhizomes of the *curcuma longa* plant, and has an intense yellow pigment. In addition to its analgesic, wound healing, antioxidant, antidiabetic, antihypertensive, antihepatotoxic, antipsoriasis, antimicrobial, antifungal, anti-inflammatory, antiproliferative and antiangiogenic properties [13–15], it presents a potent effect against cervical cancer [16–18]. However, curcumin has limited clinical application since it is poorly water soluble, has a low half-life and is chemically instable, which decreases its bioavailability and consequently its therapeutic action [19]. In order to increase its bioavailability, curcumin can be loaded in drug delivery systems [14,19].

Engineered nanoparticles are a promising tool for the development of modern drug delivery systems aiming to improve the efficiency of drug treatments and minimize their side effects [20–24]. Among various nanocarrier systems, lipidic nanoparticles possessing an internal cubic phase structure, known as cubosomes, have attracted increasing interest [25–28].

Cubosomes are stable colloidal dispersions, have sizes ranging from 100 to 300 nm, and exhibit a complex nanostructure [28,29]. They are characterized by a bicontinuous lipid bilayer extending in three dimensions and two interwoven, but unconnected, aqueous nanochannels. Three main structures of bicontinuous cubic phases can be identified: the diamond (Pn3m), the primitive (Im3m), and the gyroid (Ia3d) [29,30]. Cubosomes offer several advantages, such as the ability to improve drug bioavailability and reduce drug toxicity [31,32], to encapsulate hydrophilic as well as hydrophobic drugs, and protect them against physical andchemical degradation and enable their controlled release

[25,33–35]. Furthermore, this system allows the administration of drugs by safer and more effective routes with minimal toxicity, such as the topical route [29].

In this study, we incorporated curcumin into cubosomes with the objective of facilitating its use for the topical treatment of cervical cancer. The developed cubosomes were composed of (Monoolein) MO, DOTAP, Pluronic® F127, and acetate buffer (Fig. 1). Their structure and stability were characterized by SAXS, DLS, and cryo-TEM techniques. The permeation and retention of curcumin were evaluated *ex vivo*, the cytotoxicity and cellular uptake were evaluated *in vitro*, and the antiangiogenic effect was verified using the chick embryo chorioallantoic membrane (CAM) model. The results showed that curcumin is successfully incorporated into the cubosomes, which delivered and retained the drug in the vaginal mucosa. In addition, the curcumin-loaded cubosomes exhibited antiangiogenic activity, decreasing the number and diameter of blood vessels in the CAM model. This study suggests that cubosomes are a potential nanotechnological platform capable of improving the vaginal bioavailability of lipophilic drugs, such as curcumin, and enhancing topical cervical cancer treatment.

2. Materials and methods

2.1. Materials

1-Monooleoyl-*sn*-glycerol C18:1 (monoolein, MO) > 99% was purchased from Nu-Chek Prep, Inc., U.S.A. DOTAP > 99% was purchased from Cordenpharma, Switzerland. Pluronic® F127 > 99% was purchased from BASF, U.S.A. Acetonitrile (HPLC grade) was purchased from J.T. Baker, U.S.A., and chloroform $\geq$ 99.8% was purchased from Merck, Germany. Ethanol 99.5%, methanol 99.8%, and sodium acetate trihydrate > 99% were purchased from Sigma Aldrich, Brazil. Propylene glycol $\geq$ 99.5% and acetic acid $\geq$ 99% were purchased from Synth, Brazil. Span 60 45 – 55% was purchased from Audaz, Brazil, and curcumin $\geq$ 65% was purchased from Sigma Aldrich, Switzerland. All solutions were prepared using Mili-Q water (18.2 MΩ cm^{-1}; Millipore, U.S.A.). Sephadex PD MiniTrap™ G-25 column was purchased from Sigma Aldrich, Switzerland. CellTox™ Green Cytotoxicity Assay kit and Apo-ONE® Homogeneous Caspase-3/7 Assay kit were purchased from Promega Madison, U.S.A. MitoTracker® Red and DAPI were purchased from Vector Laboratories Inc., U.S.A.

2.2. Development of cubosomes

Cubosomes were formed by adapting the protocol described by Martiel et al. (2015) [36]. MO, DOTAP and curcumin were weighed in a tube, and the components for each formulation are reported in Table 1. The lipids with or without curcumin were dissolved in chloroform, and then the co-solvent was evaporated in a rotary evaporator to provide a lipid film. After overnight storage in a desiccator under reduced pressure, the film was hydrated with a solution containing acetate buffer pH 4.4 and Pluronic® F127 1.5%. The formulation was vortex-mixed and sonicated at 45% amplitude in a cycle of 0.8 s on/0.8 s off for 5 min to obtain monodispersed cubo-
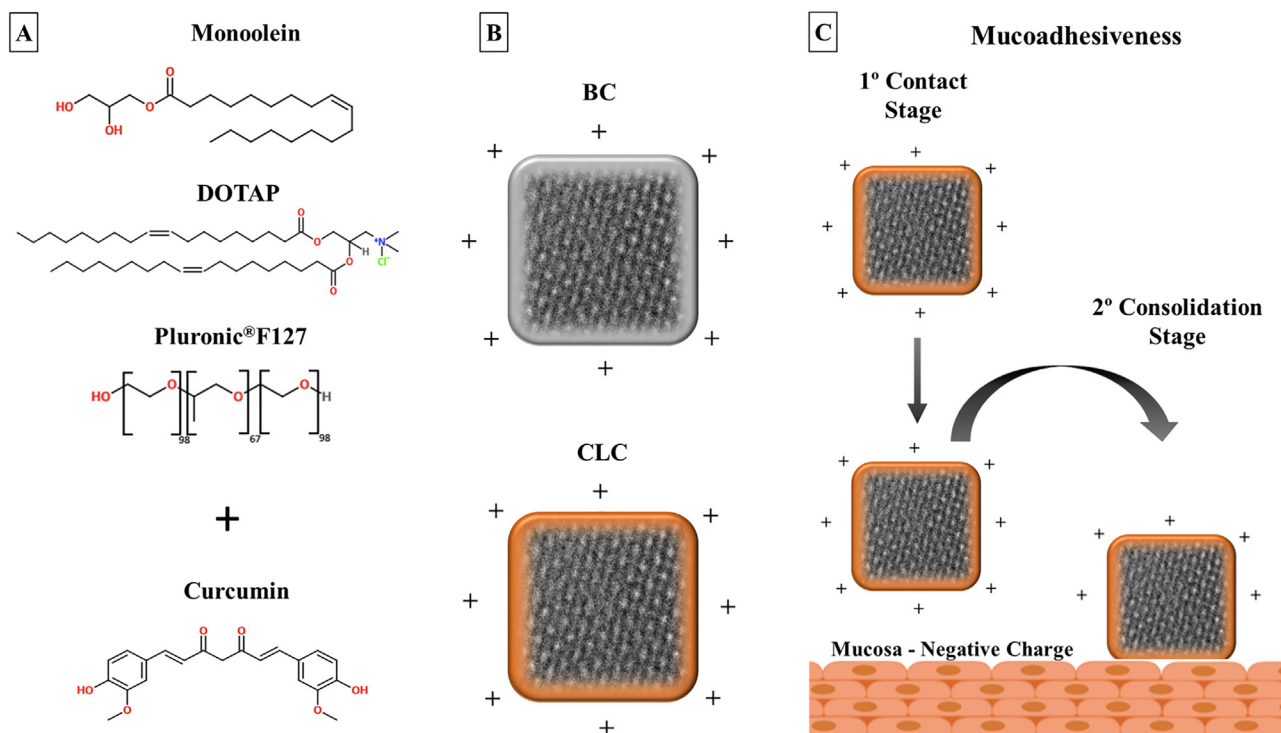
Fig. 1. Study outline. (A) Components of the cubosomes, (B) blank cubosomes (BC) and curcumin-loaded cubosomes (CLC), and (C) the interaction of the cubosomes with the negatively-charged mucosa.

Table 1
Nomenclature and composition of formulation.

Formulations	Monoolein	Curcumin	DOTAP	Acetate buffer
BC	9.5%	–	0.5%	90%
CLC	9.4 – 9.0%	0.1 – 0.5%	0.5%	90%

somes. Curcumin was incorporated in the concentrations of 5 mg/mL or 1 mg/mL.

2.3. Small-angle X-ray scattering (SAXS)

SAXS measurements were performed to determine the internal nanostructure of the lipidic nanoparticles. We used a Bruker AXS Micro instrument with a microfocused X-ray source, operating at 50 kV and 1000 μA. The Cu Kα radiation (λCu Kα = 1.5418 Å) was collimated by a 2D Kratkycolimator, and the data were collected by a 2D Pilatus 100 K detector. The scattering vector q = $(4 \pi/\lambda) \sin\theta$, with 2θ being the scattering angle, was calibrated using silver behenate. Data were collected and azimuthally-averaged using the Saxsgui software to produce unidimensional intensity versus scattering vector q, with a q interval of 0.004 to 0.4 Å^{-1}. The measurements were performed at 25 °C, which was the room temperature considered for the administration of the formulation to the patient, and at 37 °C, the temperature of the vaginal mucosa. The scattering intensity was collected for 2 h.

2.4. Cryo-transmission electron microscopy (cryo-TEM)

For cryo-TEM, grids were prepared in a controlled environment vitrification system Vitrobot Mark IV (Thermo Fisher Scientific, U.S.A.) kept at 22 °C with humidity close to saturation to prevent evaporation during preparation. A droplet of the cubosomes, diluted 5 × in MilliQ, was placed onto a hydrophilized lacey carbon-

coated copper grid (Quantifoil, D), gently blotted with filter paper to remove excess liquid, and immediately submerged into liquid ethane/propane for vitrification. The grid was stored in liquid nitrogen and transferred into a Tecnai F20 transmission electron microscope (Thermo Fisher Scientific, U.S.A.) operated at 200 kV in bright-field mode. Digital images were recorded under low dose conditions with a Falcon II direct electron detector (Thermo Fisher Scientific, U.S.A.).

2.5. Hydrodynamic diameter and polydispersity evaluation

The mean hydrodynamic diameter, polydispersity index and zeta potential of cubosomes were measured at 25 °C and 37 °C, through dynamic light scattering, using a Zeta Sizer Nano ZS (Malvern Instruments, Malvern, U.K.).

2.6. Encapsulation efficiency of curcumin-loaded cubosomes

Excess nonincorporated curcumin was separated from the cubosomes by size exclusion chromatography using a Sephadex PD MiniTrap™ G-25 column. Two protocols were performed: a gravity protocol, which was used to prepare the formulation employed in *ex vivo* permeation and retention studies, and to evaluate the vascular response using the CAM model; and a spin protocol, which was used to prepare the formulation employed in *in vitro* cytotoxicity and cellular uptake assays. Gravity protocol: approximately 0.2 mL of formulation with 5 mg/mL was added

to the Sephadex column, and eluted using acetate buffer pH 4.4 as the mobile phase. The eluted fractions were monitored by turbidity measurements at 425 nm using a microplate reader (Tecan, Austria). Approximately 60 fractions were collected. Then, the fractions with similar turbidity were joined and solubilized in ethanol, and the curcumin concentration was analyzed in a microplate reader at 425 nm. Spin protocol: approximately 0.5 mL of formulation with 1 mg/mL was added to the Sephadex column, and eluted by centrifugation at 1000 RCF (Labgene Scientific, Switzerland). The encapsulated curcumin was measured at 425 nm using a microplate reader (Tecan, Austria). The concentration of the solution added in the Sephadex column was considered 100%, and the concentration obtained after elution in the fractions corresponding to the encapsulated curcumin was compared with this value, resulting in the encapsulation efficiency of curcumin in cubosomes.

2.7. Ex vivo permeation and retention studies

The *ex vivo* permeation and retention studies of the control, composed of free curcumin in acetate buffer and incorporated curcumin into the cubosomes, were performed using Microette (Hanson, U.S.A.) equipment consisting of Franz diffusion cells. In these experiments, a receptor solution composed of acetate buffer pH 4.4 with 15% propylene glycol, 5% ethanol and 1% Span® 60 at 37 °C and under stirring at 300 rpm, was used with adaptations according to Rodero et al. (2018) [37]. A porcine vaginal mucosa prepared as described by DosSantosRamos et al. (2016) [38] was used. The samples were placed on the vaginal mucosa at the donor compartment of the Franz diffusion cell. The amount of curcumin permeated through the mucosa was collected automatically after 5 min, 10 min, 30 min, 1 h, 2 h, 4 h, 6 h, 8 h, and 12 h, and quantified using high performance liquid chromatography (HPLC, Agilent, Japan) with a wavelength of 425 nm. The quantification was performed using a column type C18, 4.6 mm × 250 mm (Symmetry, U.S.A) 5 mm; flow, 1.2 mL/min, and acidified water with 2% acetic acid and acetonitrile 50:50 (v/v) as eluent. The calibration curve was determined from a standard curcumin solution of 0.5–70.0 µg/mL according to the analytical method validated by Fonseca-Santos et al. (2017) [39]. Curcumin retained in the porcine vaginal mucosa was extracted according the method adapted from Victorelli et al. (2018) [40]. After 12 h, the mucous membranes were cleaned using soft paper and cut into small fragments. The cut mucosa was placed in 15 mL centrifuge tubes (BD Falcon®, U.S.A.) containing 4 mL of methanol, and ground in Turrax® at 10.000 rpm for 2 min. Then, the tubes were immersed in an ultrasonic bath for 30 min. The supernatant was filtered, and the amount of curcumin was quantified by HPLC, using the same method described above and through the calibration curve in methanol.

2.8. In vitro cytotoxicity assay

2.8.1. Cells and culture conditions
HeLa cell line (purchased from American Type Culture Collection, ATTC®, U.S.A., and provided by Euroclone, Italy) was cultured in DMEM medium supplemented with 10% fetal bovine serum, 1% L-glutamine, and 1% penicillin/streptomycin. Cell culture was kept at 37 °C with a humidified atmosphere of 5% CO_2.

2.8.2. Cytotoxicity and apoptosis assays
The CellTox™ Green Cytotoxicity Assay kit was used to quantify cytotoxicity, and the Apo-ONE® Homogeneous Caspase-3/7 Assay kit was employed to determine apoptosis in treated cells as previously described [41,42]. Fluorescence was determined by a Glo-

Max® Discover Microplate Reader instrument (Promega Madison, U.S.A.).

2.9. In vitro cellular uptake

HeLa cells were seeded onto a 6-well coverglass (Thermo Fisher Scientific Inc., U.S.A.) at a density of 15×10^4 /well. After 24 h, the initial medium was replaced by a fresh medium containing free curcumin or curcumin-loaded cubosomes. After 1.5 h, mitochondria and cellular nuclei were stained as previously described [41] with MitoTracker® Red, DAPI, and Vectashield as mounting medium. Caspase activity was expressed as relative fluorescence unit (RFU), measured after 30 min by the Glomax MultiDetection System (Promega Madison, U.S.A.). The fluorescent images were captured using the Cytation 5 cell imaging multi-mode reader with objective lens 10 × or 60 ×, and processed by GEN.5 software (Bio-Tek, Germany).

2.10. Evaluation of vascular response using the CAM model

This study was approved by the Ethics Committee on the Use of Animals of the Sao Carlos Institute of Physics - University of São Paulo (CEUA/IFSC) under protocol number 9261230819. Chicken eggs were donated by local producers (Mario Salviato - Ovos Férteis Porto Ferreira/SP, Brazil and AD'ORO S.A., São Carlos/SP, Brazil). The assays were performed with adaptations according to Buzza et al. (2019) [43]. On the first day of embryo development (ED1), the eggs were cleaned with 70% alcohol and incubated at 37.7 °C with approximately 60% humidity, in constant slow rotation motion - half cycle each 30 min. A window of approximately 2 cm² was opened in the thinnest part of the shell on ED4. Subsequently, using a syringe and a needle, approximately 3 mL of albumin was extracted from the egg, and then the window was sealed with adhesive tape. The eggs were returned to the incubator and the assay started on ED7, when the blood vessels reached the appropriate size for analyses. All procedures were performed inside of a laminar flow hood to avoid contamination. The dilution of the formulation was based on the effective concentration range of CLC in the CAM model. Considering 1 mg/mL the concentration of the curcumin in CLC, the samples were diluted 10 × (0.1 mg/mL curcumin) and 25 × (0.04 mg/mL of curcumin). For the assessment of vascular changes in CAM, on ED7, 50 uL of the formulations BC and CLC diluted 10 × and 25 × were added to the CAM. A USB Digital Microscope® (Avant-Garde, China) was used, and the images were captured prior to treatment and after 4 h and 24 h. For the quantitative analysis, the number of nodes that comprise at least three branches was determined with Image J software.

2.11. Statistical analysis

The significance of the effect of the formulation on curcumin retention (%) was evaluated by two-tailed Student's *t*-test. The effects of formulations (blank cubosomes and curcumin-loaded cubosomes) and temperature (25 °C and 37 °C) on particle size and polydispersity index of cubosomes were analyzed using two-way ANOVA (post hoc by Bonferroni). These analyses were performed using IBM Statistics 26 software. For the *in vitro* cytotoxicity assay results, the statistical analyses were performed using an unpaired two-tailed Student's *t*-test. The analyses with *p* values < 0.05 at a 95% confidence interval were considered significantly different.

3. Results and discussion

Cubosomes are composed of biodegradable and biocompatible lipids, e.g., glyceryl monooleate (monoolein, MO) [28], dispersed in water with the aid of a polymer stabilizer, such as Pluronic® F127 [27]. Monoolein is an amphiphilic lipid due the presence of a polar head group and a non-polar hydrocarbon chain (Fig. 1A) [44] that self-assembles in water to form liquid crystalline phases, including the bicontinuous cubic phase that can be dispersed to form cubosomes [27,30,45]. Monoolein is widely utilized in the pharmaceutical and food industries, since it is considered nontoxic, biodegradable, biocompatible, and reported in the FDA's Inactive Ingredients Guide [34,46]. Pluronic® F127 is a linear, nonionic, water-soluble triblock polymer that contains a hydrophobic polypropylene oxide (PPO) between two hydrophilic blocks of polyethylene oxide (PEO) (Fig. 1A) [47], and acts as a hydrotope and stabilizing agent [48,49]. 1,2-dioleoyl-3-trimethylammonium-propane (DOTAP) is a cationic lipid, which was used in the development of cubosomes to give adhesive properties to the formulation [50]. The cationic charge of the lipid increases the attraction of the formulation with negatively-charged surfaces, such as the vaginal mucosa [51,52], optimizing the topical administration of cubosomes to the vaginal track (Fig. 1C).

3.1. Structural stability

The SAXS analysis of curcumin-loaded and unloaded cubosomes is shown in Fig. 2 at room temperature 25 °C and vaginal mucosa temperature 37 °C. The scattering curves of blank (Fig. 2A) and curcumin-loaded cubosomes (Fig. 2B) are very similar, as both exhibited the primitive cubic phase (Im3m) at 25 °C and 37 °C, confirming that the incorporation of curcumin in the cubosomes does not affect their internal nanostructure. The Im3m unit lattice parameters estimated for blank cubosomes were 160.78 Å and 152.54 Å, and for curcumin-loaded cubosomes were 157.82 Å and 152.43 Å at 25 °C and 37 °C, respectively. The lattice parameter of both samples decreased with increasing temperature, as the curvature of the lipid system decreases at higher temperatures [53]. The nanostructure is also confirmed by cryo-transmission electron microscopy (cryo-TEM) (Fig. 2C and D), which shows the presence of cubosomes and vesicles, which are typically formed in monoolein dispersions [54,55].

3.2. Size, zeta potential and encapsulation efficiency

The mean hydrodynamic diameter, polydispersity index (PDI) and zeta potential (ξ) of the cubosomes were analyzed at 25 °C and 37 °C by dynamic light scattering (DLS), and the results are presented in Fig. 3. Particles with a homogeneous size distribution with a PDI lower than 0.4 [56,57] were formed. The nano-sized particles and the internal nanostructure create a large surface area that is ideal to optimize drug delivery [58,59]. In addition, nanometric sizes strongly influence the ability of cells to recognize and internalize nanoparticles [60]. The increase of temperature to 37 °C increased the PDI and the particles' diameter. Nevertheless, as the particles stayed nanometric and the PDI was below 0.4, the system remained suitable for the application. Zeta potential measurements confirm the positive charge of the systems.

The nature of the systems and the characteristics of the drug influence the efficiency of encapsulation [61]. We quantified the encapsulation efficiency by size exclusion chromatography. For the formulation with 5 mg/mL of curcumin, the encapsulation efficiency was approximately 20.2%. The encapsulation efficiency was successfully increased to 86%, reducing the concentration of curcumin to 1 mg/mL.

3.3. Ex vivo permeation and retention studies

The permeation and retention of curcumin-loaded cubosomes in contact with vaginal mucosa were investigated. The vaginal mucosa is characterized by an epithelial layer, the surface of which is covered by mucus. The mucus contains lipids, inorganic salts, glycoproteins, 95% water, and has a negative net charge [51,52].

The first step of mucoadhesion is contact between the system and the vaginal mucosa. The second step is consolidation, in which the system and the glycoproteins of the mucus mutually interact [52,62]. This interaction can be driven by electrostatic forces, as both mucoadhesive and biological materials possess opposing electrical charges and are capable of attracting each other [52,63]. The developed cubosomes constitute positively-charged systems [50], which increase the mucoadhesion [52] (Fig. 1C), leading to longer contact time between the system and the mucosa, which prolongs drug absorption and its effects [64].

The vaginal mucosa presents tight junctions, adherens junctions, and desmosomes that may hamper the permeability of the drugs [65,66]. Free curcumin dissolved in acetate buffer was employed as a control system. Both free curcumin and curcumin-loaded cubosomes did not permeate through the vaginal mucosa, showing that the diffusion of curcumin is limited. This is an important result, since the focus of the study is local, allowing a selective effect at the application site and not on a systemic treatment. As curcumin is a lipophilic drug, it precipitates in the acetate buffer, which impedes its absorption in the mucosa. This poor solubility causes low bioavailability and consequently low therapeutic effects [67].

Approximately 5.7% of free curcumin and 8.6% of curcumin-loaded cubosomes were retained on the vaginal mucosa (Fig. 4). The retention of curcumin in cubosomes is increased by nearly 50% compared to the free curcumin ($p < 0.0001$). A greater retention may have been modulated by the presence of DOTAP in the formulation, which is a cationic lipid that increases the attraction to the vaginal mucosa [50,52], and improves the cubosomes mucoadhesion and, in turn, the retention of the drug.

Although the curcumin released from the cubosomes did not permeate the vaginal mucosa, it was retained in the membrane. This observation suggests that the interaction of curcumin in the vaginal environment would occur mainly in the mucosa, being limited in deeper layers. Therefore, such curcumin-loaded cubosomes are ideal for topical use, in which a local effect is desired [68]. Our system is capable of solubilizing lipophilic drugs and releasing them in the outer layers for the topical treatment of vaginal diseases.

3.4. In vitro cytotoxicity assay

HeLa cells were exposed to different isoconcentration solutions of free curcumin and curcumin-loaded cubosomes with a concentration range of 5–100 μM for 24 h of exposure. As a control, cells were exposed to blank cubosomes (206.5 – 4130.4 μg/mL monoolein) (Fig. 5A). We then investigated the cell viability and the caspase 3/7 activity (Fig. 5B) in Hela cells, i.e., our toxicity model. Cell viability and caspase 3/7 activity were not affected by blank cubosomes at the examined concentration range, demonstrating the high biocompatibility profile of the system. The system developed is highly concentrated and consists of 95,000 μg/mL of monoolein. We could observe that when applying the system to the HeLa cells at a monoolein concentration of approximately 4,000 μg/mL, the higher concentrated nanoparticles accumulated on the cell membranes, forming a layer, and the nanoparticle internalization was saturated [69–71]. This may explain why the high concentration of monoolein was not toxic to this cell line, since the cells could not internalize all of the nanoparticles available. In contrast, cubo-
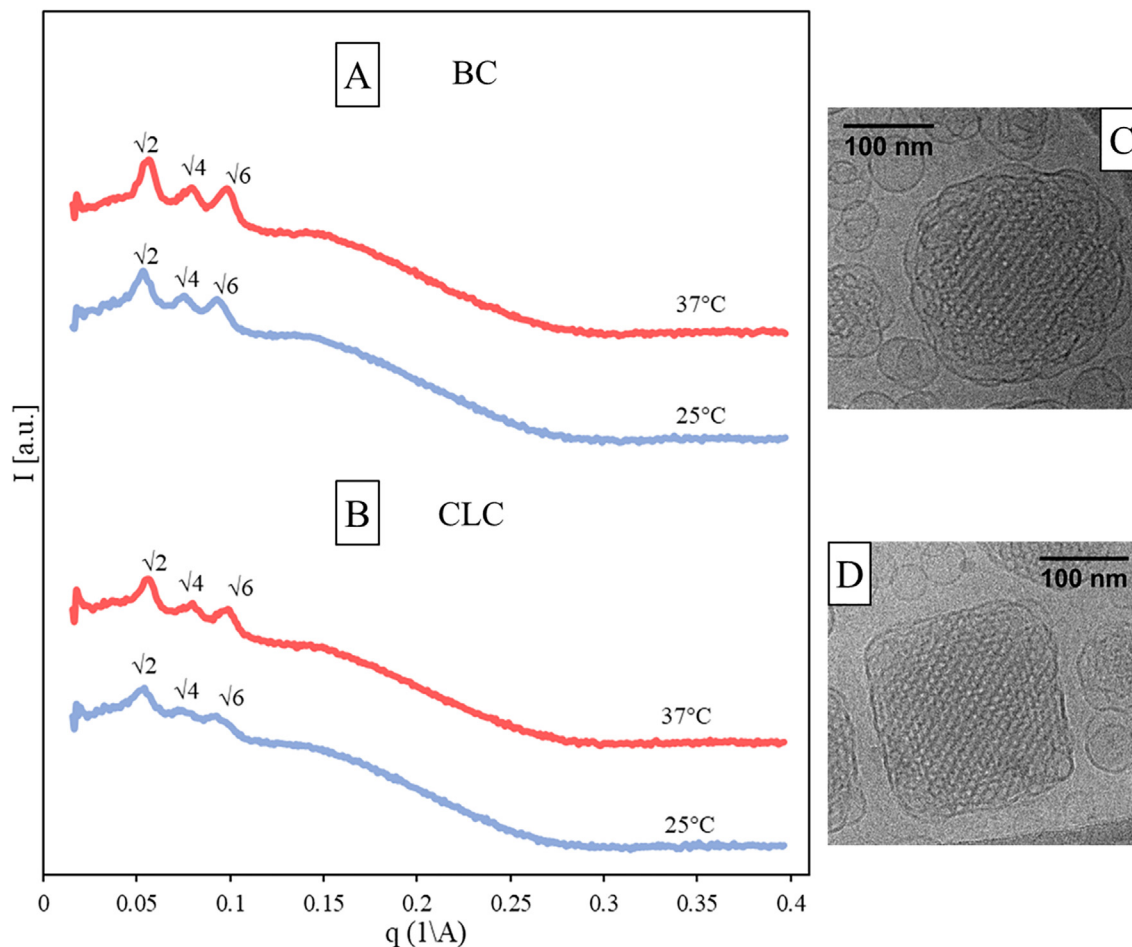
Fig. 2. (A) SAXS curve of blank cubosomes (BC) (B) SAXS curve of curcumin-loaded cubosomes (CLC) (C) cryo-TEM of blank cubosomes (BC) (D) cryo-TEM of curcumin-loaded cubosomes (CLC).
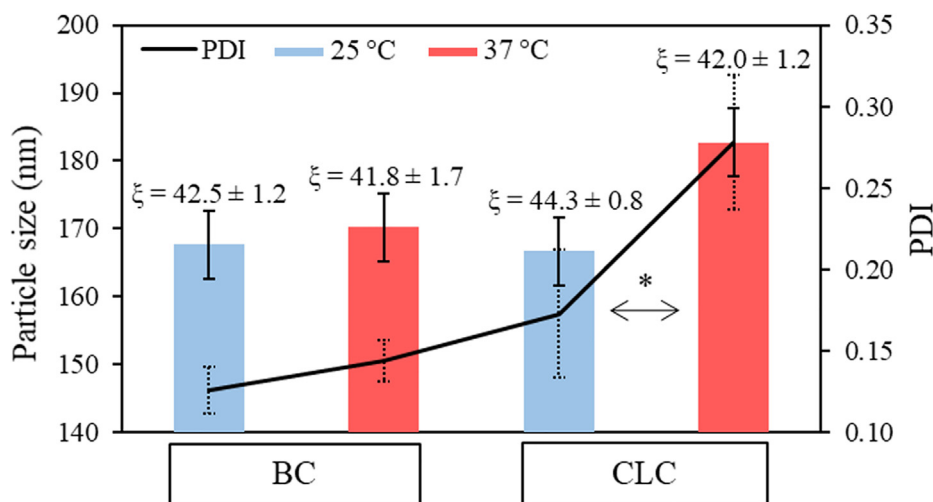

Fig. 3. Hydrodynamic diameter, PDI and zeta potential (ξ) of blank cubosomes (BC) and curcumin-loaded cubosomes (CLC) at 25 °C and 37 °C. *Denotes statistical differences between groups, two-way ANOVA, Bonferroni (n = 9: n = 3 in three different replications *p < 0.0001).

somes with the same monoolein concentration and loaded with curcumin are cytotoxic to HeLa cells, indicating that the cytotoxicity is caused by curcumin. Curcumin-loaded cubosomes produced a statistically significant dose-dependent toxicity with an increase in cell mortality from 6.34% (*p*-value = 1,65604E-05) to 100% (*p*-value = 3,80262E-08) for HeLa cells, as curcumin is able to cause apoptosis in this cell line [72,73]. Cells treated with free curcumin showed a markedly reduced toxicity compared to the curcumin-equimolar cubosomes formulation, with a mortality of less than 20% over the concentration range tested (Fig. 5A). Curcumin-
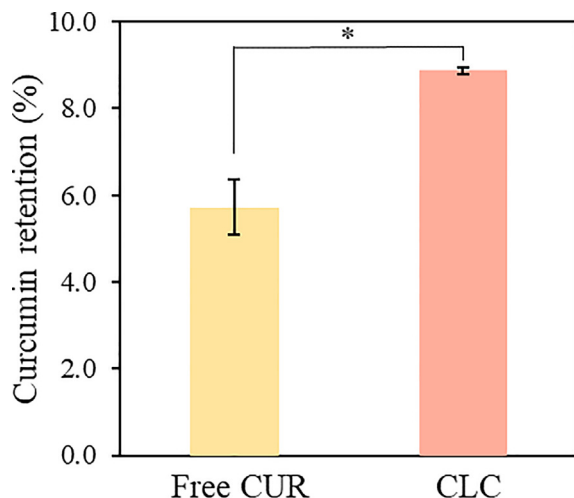
Fig. 4. Curcumin retention from free curcumin and curcumin-loaded cubosomes (CLC). *Denotes statistical differences between formulations, unpaired t-tests (*$p < 0.0001$, n = 3).

loaded cubosomes exhibited significantly higher caspase 3/7 activity than free curcumin (Fig. 5B). This may occur because the cubosomes fuse with the lipidic membrane of the cell [74] and are able to release curcumin into HeLa cells, as can be seen in the *in vitro* cellular uptake. These results indicate that the incorporation of curcumin into developed cubosomes contributed to increase the drug's bioavailability, thus improving the effectiveness of the treatment.

3.5. In vitro cellular uptake

We performed a microscopy analysis to compare the cellular uptake of curcumin-loaded cubosomes with free curcumin. HeLa cells were exposed for 1.5 h to the formulation solution at a concentration of 50 μM, and then fixed. As shown in Fig. 5C, the curcumin gave a stronger signal in cells treated with curcumin-loaded cubosomes than in cells treated with free curcumin. The developed cubosomes comprise a cationic lipid (DOTAP) in their composition, and it may allow the nanoparticles to have more intense contact with the cells with negatively-charged outer cell membranes. A strong cell adhesion increases the retention of nanoparticles at the site of administration and may allow a depot effect of nanoparticles around the cell. This process increases the exposure time of curcumin to cancer cells and improves its entry into the cell [74–77], enhancing intracellular drug accumulation and consequently treatment efficacy. The effects of curcumin-loaded cubosomes on cell morphology were consistent with their reported ability to cause cell death, as shown in the bright field images. Control and curcumin-treated cells' mitochondria looked like structures forming a regular network in perinuclear positions. In contrast, after curcumin-loaded cubosomes treatment, mitochondria formed more heterogeneously-distributed clusters, indicating that the cells underwent apoptosis [78]. This result strengthens the results obtained in the *in vitro* cytotoxicity experiment discussed above, confirming the increased efficiency of the treatment of cervical cancer with curcumin-loaded cubosomes.

3.6. Application of curcumin-loaded cubosomes in the chorioallantoic membrane (CAM) model

Angiogenesis is the process of forming new blood vessels from pre-existing ones [79] and it is stimulated by angiogenic factors, such as vascular endothelial growth factor (VEGF). This process

occurs in physiological conditions, but several diseases are also associated with abnormal angiogenesis, such as inflammatory and infectious disorders and tumor [79–81]. Curcumin is able to inhibit the induction pathways of the pro-angiogenic factor FGF-1, and acts as an antiangiogenic drug [82]. To evaluate the angiogenic activity of drugs and drug delivery systems, the chick embryo chorioallantoic membrane (CAM) has been a widely used model [43,83–85]. The CAM is an extraembryonic membrane that is formed during chick embryo development and presents a rich vascular system, which allows the visualization of pro and antiangiogenic effects [86].

As an example of application, we tested the capacity of the curcumin-loaded cubosomes to decrease the angiogenic effect by the CAM model. Buzza et al. (2019) [43] studied the antiangiogenic effect of curcumin in this model and they verified that curcumin exhibits a vascular effect related to its angio-inhibitory effect. The CAM model provides a rapid method for investigating the release of curcumin in a biological system and the antiangiogenic activity of the formulation. However, there are few studies in the literature that verified the anti-angiogenic effect of curcumin-loaded drug delivery by the CAM model. To the best of the authors' knowledge, this study is the first example reported in the literature of angiogenesis inhibition induced by curcumin-loaded cubosomes. Yadav et al. (2009) [83] developed solid lipid microparticles with curcumin, and revealed a vascular regression using free curcumin and the system developed. Mandracchia et al. (2016) [87] showed that curcumin-loaded inulin-vitamin E micelles (INVITE) presented an antiangiogenic affect. Sethuraman et al. (2019) [88] reported that lumefantrine with calcium phosphate nanoparticle-loaded cubosomes presented a better antiangiogenic effect than pure lumefantrine, showing that cubosomes may potentialize the antiangiogenic effect of drugs.

The vascular network grows during embryonic development, and this growth may increase or decrease in response to specific stimuli [89]. The effect of the samples was analyzed qualitatively (visually) and quantitatively, using the branch counting methodology [89]. The formulations BC and CLC, when tested at the initial concentration (standard formulation – 1mg/mL curcumin), showed such an exacerbated effect that they led to the embryo's death, which indicates that the concentrated formulations are highly toxic, regardless of the presence of curcumin. Thus, looking for a lower concentration that would not cause death to the embryo, the formulations were diluted 10 and 25 times.

In the 10 × dilution, the blank cubosomes (BC) caused an increase in the number of the vessels, resulting from dilation of large vessels and destruction of small ones (Fig. 6.1A). Despite this toxic effect, all embryos remained alive, which allowed analysis for up to 24 h. Using curcumin-loaded cubosomes (CLC), the effect on the vessels was much more evident both qualitatively (Fig. 6.1B) and quantitatively (Fig. 6.2A) and, therefore, we assumed that this severe effect of the CLC compared to the BC was due to the antiangiogenic effect of curcumin. The quantitative results (Fig. 6.2A) also suggest that both samples BC and CLC presented some toxicity effect, as the vascular network increased after 4 h. After 24 h, however, the vascular network decreased but remained denser compared to the control. Nevertheless, it is clear in the images of Fig. 6.1A and 6.1B that these vessels are malformed, not being considered healthy vessels. This toxicity effect could be attributable to the presence of DOTAP and Pluronic® 127. The cationic lipid presents a quaternary amine headgroup that could be responsible for the inhibition of protein kinase C, which may be associated with their toxicity [90]. Moreover, Pluronic® 127 may produce some inflammation, since it activates the complement of the immune system [41]. Therefore, as the blank cubosomes caused changes in the vascular network, it was still necessary to increase the dilution to analyze the real effect of curcumin.
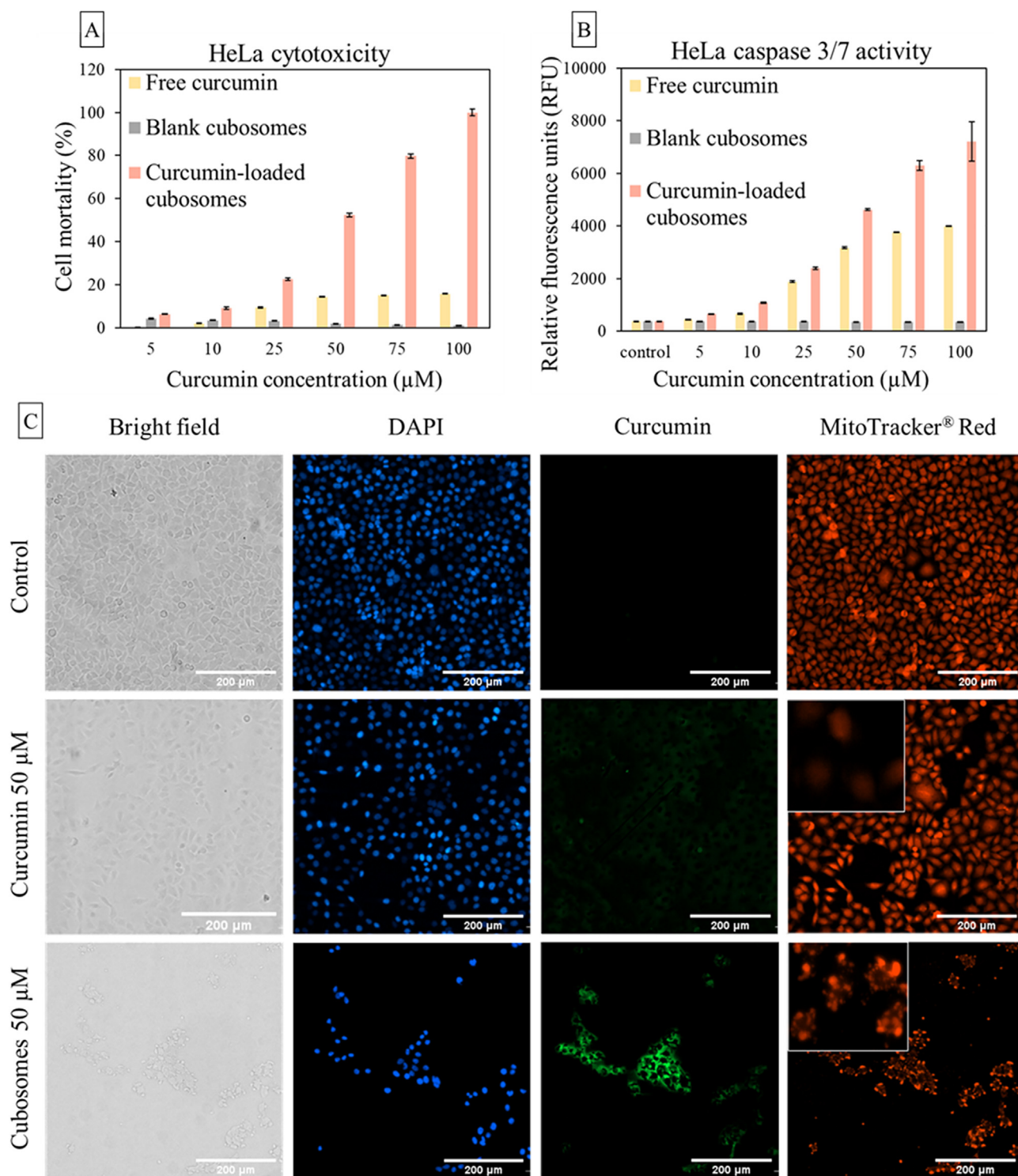
Francesca Damiani Victorelli, L. Salvati Manni, S. Biffi et al.

Journal of Colloid and Interface Science 620 (2022) 419–430

Fig. 5. Cytoxicity assessment and cellular uptake of the free curcumin and curcumin-loaded cubosomes by HeLa cell line. (A) Cellular mortality of HeLa cells incubated with formulations at different concentrations for 24 h. Data are shown as mean ± SD of three individual experiments. (B) Effects on caspase 3/7 activity in HeLa cells induced by treatment with different formulations. (C) Fluorescence microscopy images of cellular uptake by HeLa cells of free curcumin and curcumin-loaded cubosomes. The first column represents the bright field, the second column DAPI staining (nuclei, blue), the third columnthe curcumin fluorescence emission of the free curcumin and curcumin-loaded cubosomes treated cells, and the last column MitoTracker® labelling (mitochondria, red). Scale bar 200 μm, insert 30 μm. (For interpretation of the references to colour in this figure legend, the reader is referred to the web version of this article.)

Effectively, when the blank cubosomes were diluted 25 ×, almost no toxicity or antiangiogenic effects were observed after 24 h in all replicates, as shown in Fig. 6.1C. This behavior indicated that this dilution was ideal for analyzing the antiangiogenic effect of curcumin-loaded cubosomes by the CAM model. Fig. 6.1D shows

that the CLC diluted 25 × presented a decrease in the number and the diameter of the vessels, suggesting again that the curcumin released from the cubosomes was able to impart an antiangiogenic effect. The quantitative results confirmed the qualitative results for the 25 × diluted samples, even with a mild effect. The graph in
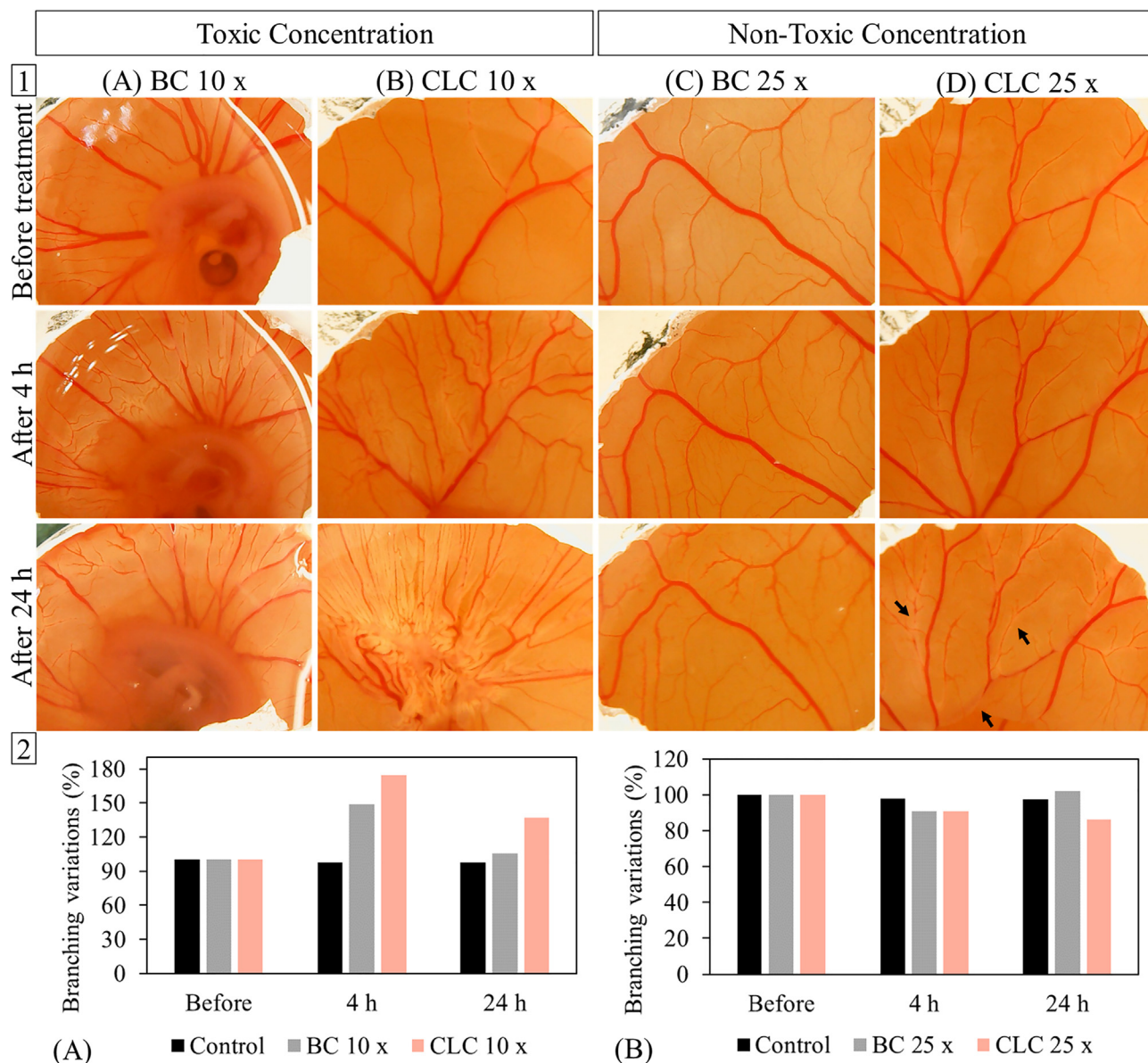
Fig. 6. 1- Qualitative angiogenic effect: (A) blank cubosomes (BC) diluted 10 ×, (B) curcumin-loaded cubosomes (CLC) diluted 10 ×, (C) blank cubosomes (BC) diluted 25 ×, (D) curcumin-loaded cubosomes (CLC) diluted 25 ×. 2- Quantitative angiogenic effect: (A) blank cubosomes (BC) diluted 10 × and curcumin-loaded cubosomes (CLC) diluted 10 ×, (B) blank cubosomes (BC) diluted 25 × and curcumin-loaded cubosomes (CLC) diluted 25 ×.

Fig. 6.2B shows that CLC 25 × decreased the vascular network compared with the control and BC 25 ×. Therefore, it can be seen that the curcumin-loaded cubosomes should be an effective system to decrease the angiogenic effect caused by several diseases.

4. Conclusion

Lipidic nanoparticles with an internal cubic nanostructure, known as cubosomes, were designed with DOTAP, a cationic lipid, to improve the mucoadhesion and allow the vaginal application of lipophilic drugs, such as curcumin, for the topical treatment of cervical cancer. The curcumin-loaded cubosomes were characterised with SAXS, cryo-TEM, and DLS. They exhibited nanometric size, homogeneous hydrodynamic diameter, and Im3m nanostructure. The curcumin released from the cubosomes was retained in the vaginal epithelium, showing that the system has potential for topical administration. *In vitro* cytotoxicity and cellular uptake assays

demonstrated that Hela cells were able to internalize the cubosomes, and that these nanoparticles enhanced the curcumin's effect against cervical cancer cells. Although the concentration of cubosomes used in this study may be too high for systemic administration, the efficacy of the proposed approach may be ideal for depot application. The *in vivo* study using the CAM model showed that the curcumin-loaded cubosomes presented antiangiogenic activity, reducing the diameter and number of blood vessels after 4 h of treatment. These promising results confirm that our cubosomes constitute a highly promising platform for the incorporation of lipophilic drugs for the topical treatment of cervical cancer. Moreover, compared to other developed cubosomes [26,91,92] the present investigation brings a strategy to design mucoadhesive cubosomes and improve the vaginal application of lipophilic drugs. As future work, we suggest performing *in vivo* cancer model assays to better understand the behavior and efficiency of the cubosomes in the vaginal environment.

Declaration of Competing Interest

The authors declare that they have no known competing financial interests or personal relationships that could have appeared to influence the work reported in this paper.

Acknowledgements

Data availability

Data are available from the corresponding author upon reasonable request.

References

[1] K.P. Medina-Alarcón, A.R. Voltan, B. Fonseca-Santos, I.J. Moro, F. de Oliveira Souza, M. Chorilli, C.P. Soares, A.G. dos Santos, M.J.S. Mendes-Giannini, A.M. Fusco-Almeida, Highlights in nanocarriers for the treatment against cervical cancer, Mater. Sci. Eng. C. 80 (2017) 748–759, https://doi.org/10.1016/j.msec.2017.07.021.

[2] M. Arbyn, E. Weiderpass, L. Bruni, S. de Sanjosé, M. Saraiya, J. Ferlay, F. Bray, Estimates of incidence and mortality of cervical cancer in 2018, a worldwide analysis, Lancet Glob. Heal. 8 (2020) e191–e203, https://doi.org/10.1016/S2214-109X(19)30482-6.

[3] F.D. Victorelli, M.F. Calixto, K. Cristina, D. Santos, H. Harb Buzzá, M. Chorilli, Curcumin-loaded Polyethyleneimine and chitosan polymer-based Mucoadhesive liquid crystalline systems as a potential platform in the treatment of cervical Cancer, J. Mol. Liq. 325 (2021), https://doi.org/10.1016/j.molliq.2020.115080.

[4] G.C. Carvalho, V.H.S. Araujo, B. Fonseca-Santos, J.T.C. de Araújo, M.P.C. de Souza, J.L. Duarte, M. Chorilli, Highlights in poloxamer-based drug delivery systems as strategy at local application for vaginal infections, Int. J. Pharm. 602 (2021), https://doi.org/10.1016/j.ijpharm.2021.120635 120635.

[5] A. Hussain, F. Ahsan, The vagina as a route for systemic drug delivery, J. Control. Release. 103 (2005) 301–313, https://doi.org/10.1016/J.JCONREL.2004.11.034.

[6] V.H.S. Araujo, M.P.C. de Souza, G.C. Carvalho, J.L. Duarte, M. Chorilli, Chitosan-based systems aimed at local application for vaginal infections, Carbohydr. Polym. 261 (2021) 117919.

[7] P.B. Da Silva, M.A.D.S. Ramos, B.V. Bonifácio, K.M.S. Negri, M.R. Sato, T.M. Bauab, M. Chorilli, Nanotechnological strategies for vaginal administration of drugs - A review, J. Biomed. Nanotechnol. 10 (2014) 2218–2243, https://doi.org/10.1166/jbn.2014.1890.

[8] N.J. Alexander, E. Baker, M. Kaptein, U. Karck, L. Miller, E. Zampaglione, Why consider vaginal drug administration?, Fertil Steril. 82 (2004) 1–12, https://doi.org/10.1016/J.FERTNSTERT.2004.01.025.

[9] P. Bassi, G. Kaur, Innovations in bioadhesive vaginal drug delivery system, Expert Opin. Ther. Pat. 22 (2012) 1019–1032, https://doi.org/10.1517/13543776.2012.714369.

[10] R. Salmazi, G. Calixto, J. Bernegossi, M. Aparecido Dos, S. Ramos, T.M. Bauab, M. Chorilli, A Curcumin-loaded liquid crystal precursor mucoadhesive system for the treatment of vaginal candidiasis, Int. J. Nanomedicine. 10 (2015) 4815–4824, https://doi.org/10.2147/IJN.S82385.

[11] B. Martínez-Pérez, D. Quintanar-Guerrero, M. Tapia-Tapia, R. Cisneros-Tamayo, M.L. Zambrano-Zaragoza, S. Alcalá-Alcalá, N. Mendoza-Muñoz, E. Piñón-Segundo, Controlled-release biodegradable nanoparticles: From preparation to vaginal applications, Eur. J. Pharm. Sci. 115 (2018) 185–195, https://doi.org/10.1016/j.ejps.2017.11.029.

[12] A. Lechanteur, T. Furst, B. Evrard, P. Delvenne, G. Piel, P. Hubert, Promoting Vaginal Distribution of E7 and MCL-1 siRNA-Silencing Nanoparticles for Cervical Cancer Treatment, Mol. Pharm. 14 (2017) 1706–1717, https://doi.org/10.1021/acs.molpharmaceut.6b01154.

[13] R. Carolina Alves, R. Perosa Fernandes, B. Fonseca-Santos, F. Damiani Victorelli, M. Chorilli, A Critical Review of the Properties and Analytical Methods for the Determination of Curcumin in Biological and Pharmaceutical Matrices, Crit. Rev. Anal. Chem. 49 (2019) 138–149, https://doi.org/10.1080/10408347.2018.1489216.

[14] V.H.S. Araujo, P.B. da Silva, I.O. Szlachetka, S.W. da Silva, B. Fonseca-Santos, M. Chorilli, R. Ganassin, G.R.T. de Oliveira, M.C.O. da Rocha, R.P. Fernandes, M. de Carvalho Vieira, R.B. Queiroz, L.A.M. Azevedo, The influence of NLC composition on curcumin loading under a physicochemical perspective and in vitro evaluation, Colloids Surfaces A Physicochem. Eng. Asp. 602 (2020), https://doi.org/10.1016/j.colsurfa.2020.125070 125070.

[15] M. Rakotoarisoa, B. Angelov, V.M. Garamus, A. Angelova, Curcumin- and Fish Oil-Loaded Spongosome and Cubosome Nanoparticles with Neuroprotective Potential against H 2 O 2 -Induced Oxidative Stress in Differentiated Human SH-SY5Y Cells, ACS Omega. 4 (2019) 3061–3073, https://doi.org/10.1021/acsomega.8b03101.

[16] F. Ghasemi, M. Shafiee, Z. Banikazemi, M.H. Pourhanifeh, H. Khanbabaei, A. Shamshirian, S. Amiri Moghadam, R. ArefNezhad, A. Sahebkar, A. Avan, H. Mirzaei, Curcumin inhibits NF-kB and Wnt/β-catenin pathways in cervical cancer cells, Pathol. Res. Pract. 215 (10) (2019) 152556.

[17] M.S. Zaman, N. Chauhan, M.M. Yallapu, R.K. Gara, D.M. Maher, S. Kumari, M. Sikander, S. Khan, N. Zafar, M. Jaggi, S.C. Chauhan, Curcumin Nanoformulation for Cervical Cancer Treatment, Sci. Rep. 6 (2016) 1–14, https://doi.org/10.1038/srep20051.

[18] E. Abbasifard, A. Bolhassani, S. Irani, F. Sotoodehnejadnematalahi, I.V. Balalaeva, Synergistic effects of exosomal crocin or curcumin compounds and HPV L1–E7 polypeptide vaccine construct on tumor eradication in C57BL/6 mouse model, PLoS One. 16 (10) (2021) e0258599.

[19] M. Rakotoarisoa, A. Angelova, Amphiphilic Nanocarrier Systems for Curcumin Delivery in Neurodegenerative Disorders, Medicines. 5 (2018) 126, https://doi.org/10.3390/medicines5040126.

[20] J.O. Eloy, A. Ruiz, F.T. de Lima, R. Petrilli, G. Raspantini, K.A.B. Nogueira, E. Santos, C.S. de Oliveira, J.C. Borges, J.M. Marchetti, W.T. Al-Jamal, M. Chorilli, EGFR-targeted immunoliposomes efficiently deliver docetaxel to prostate cancer cells, Colloids Surfaces B Biointerfaces. 194 (2020), https://doi.org/10.1016/J.COLSURFB.2020.111185 111185.

[21] N.N. Ferreira, S. Granja, F.I. Boni, L.M.B. Ferreira, R.M. Reis, F. Baltazar, M.P.D. Gremião, A novel strategy for glioblastoma treatment combining alpha-cyano-4-hydroxycinnamic acid with cetuximab using nanotechnology-based delivery systems, Drug Deliv. Transl. Res. 10 (2020) 594–609, https://doi.org/10.1007/s13346-020-00713-8.

[22] F.G. Prezotti, F.I. Boni, N.N. Ferreira, D.S. Silva, A. Almeida, T. Vasconcelos, B. Sarmento, M.P.D. Gremião, B.S.F. Cury, Oral nanoparticles based on gellan gum/pectin for colon-targeted delivery of resveratrol, Drug Dev. Ind. Pharm. 46 (2020) 236–245, https://doi.org/10.1080/03639045.2020.1716374.

[23] S. Aleandri, D. Bandera, R. Mezzenga, E.M. Landau, Biotinylated Cubosomes: A Versatile Tool for Active Targeting and Codelivery of Paclitaxel and a Fluorescein-Based Lipid Dye, Langmuir 31 (2015) 12770–12776, https://doi.org/10.1021/acs.langmuir.5b03469.

[24] D.J.A. Crommelin, K. Park, A. Florence, Pharmaceutical nanotechnology: Unmet needs in drug delivery, J. Control. Release. 141 (2010) 263–264, https://doi.org/10.1016/j.jconrel.2009.11.019.

[25] R. Mezzenga, J.M. Seddon, C.J. Drummond, B.J. Boyd, G.E. Schröder-Turk, L. Sagalowicz, Nature-Inspired Design and Application of Lipidic Lyotropic Liquid Crystals, Adv. Mater. 31 (2019) 1–19, https://doi.org/10.1002/adma.201900818.

[26] M. Rakotoarisoa, B. Angelov, S. Espinoza, K. Khakurel, T. Bizien, M. Drechsler, A. Angelova, Composition-Switchable Liquid Crystalline Nanostructures as Green Formulations of Curcumin and Fish Oil, ACS Sustain. Chem. Eng. 9 (2021) 14821–14835, https://doi.org/10.1021/acssuschemeng.1c04706.

[27] N. Alcaraz, Q. Liu, E. Hanssen, A. Johnston, B.J. Boyd, Clickable Cubosomes for Antibody-Free Drug Targeting and Imaging Applications, Bioconjug. Chem. 29 (2018) 149–157, https://doi.org/10.1021/acs.bioconjchem.7b00659.

[28] H.M. Abdel-Bar, R.A. el Basset Sanad, Endocytic pathways of optimized resveratrol cubosomes capturing into human hepatoma cells, Biomed. Pharmacother. 93 (2017) 561–569, https://doi.org/10.1016/J. BIOPHA.2017.06.093.

[29] Z. Karami, M. Hamidi, Cubosomes: remarkable drug delivery potential, Drug Discov. Today. 21 (2016) 789–801, https://doi.org/10.1016/J. DRUDIS.2016.01.004.

[30] A.I.I. Tyler, H.M.G. Barriga, E.S. Parsons, N.L.C. McCarthy, O. Ces, R.V. Law, J.M. Seddon, N.J. Brooks, Electrostatic swelling of bicontinuous cubic lipid phases, Soft Matter. 11 (2015) 3279–3286, https://doi.org/10.1039/c5sm00311c.

[31] Y. Chen, Y. Lu, Y. Zhong, Q. Wang, W. Wu, S. Gao, Ocular delivery of cyclosporine A based on glyceryl monooleate/poloxamer 407 liquid crystalline nanoparticles: Preparation, characterization, in vitro corneal penetration and ocular irritation, J. Drug Target. 20 (2012) 856–863, https://doi.org/10.3109/1061186X.2012.723214.

[32] Z. Yang, Y. Tan, M. Chen, L. Dian, Z. Shan, X. Peng, C. Wu, Development of amphotericin B-loaded cubosomes through the SolEmuls technology for enhancing the oral bioavailability, AAPS PharmSciTech. 13 (2012) 1483–1491, https://doi.org/10.1208/s12249-012-9876-2.

[33] J. Zhai, C. Fong, N. Tran, C.J. Drummond, Non-Lamellar Lyotropic Liquid Crystalline Lipid Nanoparticles for the Next Generation of Nanomedicine, ACS Nano. 13 (2019) 6178–6206, https://doi.org/10.1021/acsnano.8b07961.

[34] T. Madheswaran, M. Kandasamy, R.J. Bose, V. Karuppagounder, Current potential and challenges in the advances of liquid crystalline nanoparticles as drug delivery systems, Drug Discov. Today. 24 (2019) 1405–1412, https://doi.org/10.1016/j.drudis.2019.05.004.

[35] T.H. Nguyen, T. Hanley, C.J.H. Porter, B.J. Boyd, Nanostructured liquid crystalline particles provide long duration sustained-release effect for a poorly water soluble drug after oral administration, J. Control. Release. 153 (2011) 180–186, https://doi.org/10.1016/J.JCONREL.2011.03.033.

[36] I. Martiel, S. Handschin, W.K. Fong, L. Sagalowicz, R. Mezzenga, Oil transfer converts phosphatidylcholine vesicles into nonlamellar lyotropic liquid crystalline particles, Langmuir 31 (2015) 96–104, https://doi.org/10.1021/la504115a.

[37] C.F. Rodero, G.M. Fioramonti Calixto, K. Cristina dos Santos, M.R. Sato, M. Aparecido dos Santos Ramos, M.S. Miró, E. Rodríguez, C. Vigezzi, T.M. Bauab, C. E. Sotomayor, M. Chorilli, Curcumin-Loaded Liquid Crystalline Systems for Controlled Drug Release and Improved Treatment of Vulvovaginal Candidiasis, Mol. Pharm. 15 (10) (2018) 4491–4504.

[38] M.A. dos Santos Ramos, L.G. de Toledo, G.M. Fioramonti Calixto, B.V. Bonifácio, M.G. de Freitas Araújo, L.C. dos Santos, M.T.G. de Almeida, M. Chorilli, T.M. Bauab, Syngonanthus nitens Bong. (Rhul.)-loaded nanostructured system for Vulvovaginal candidiasis treatment, Int. J. Mol. Sci. 17 (2016), https://doi.org/10.3390/ijms17081368.

[39] B. Fonseca-Santos, M.P.D. Gremião, M. Chorilli, A simple reversed phase high-performance liquid chromatography (HPLC) method for determination of in situ gelling curcumin-loaded liquid crystals in in vitro performance tests, Arab. J. Chem. 10 (2017) 1029–1037, https://doi.org/10.1016/j.arabjc.2016.01.014.

[40] F.D. Victorelli, G.M.F. Calixto, M.A. Dos Santos Ramos, T.M. Bauab, M. Chorilli, Metronidazole-loaded polyethyleneimine and chitosan-based liquid crystalline system for treatment of staphylococcal skin infections, J. Biomed. Nanotechnol. 14 (2018) 227–237, https://doi.org/10.1166/jbn.2018.2484.

[41] M. Fornasier, S. Biffi, B. Bortot, P. Macor, A. Manhart, F.R. Wurm, S. Murgia, Cubosomes stabilized by a polyphosphoester-analog of Pluronic F127 with reduced cytotoxicity, J. Colloid Interface Sci. 580 (2020) 286–297.

[42] B. Bortot, M. Mongiat, E. Valencic, S. Dal Monego, D. Licastro, M. Crosera, G. Adami, E. Rampazzo, G. Ricci, F. Romano, G.M. Severini, S. Biffi, Nanotechnology-based cisplatin intracellular delivery to enhance chemo-sensitivity of ovarian cancer, Int. J. Nanomedicine. 15 (2020) 4793–4810, https://doi.org/10.2147/IJN.S247114.

[43] H.H. Buzzá, L.C.F. de Freitas, L.T. Moriyama, R.G.T. Rosa, V.S. Bagnato, C. Kurachi, Vascular effects of photodynamic therapy with curcumin in a chorioallantoic membrane model, Int. J. Mol. Sci. 20 (2019) 1–12, https://doi.org/10.3390/ijms20051084.

[44] C.V. Kulkarni, W. Wachter, G. Iglesias-Salto, S. Engelskirchen, S. Ahualli, Monolein: A magic lipid?, Phys Chem. Chem. Phys. 13 (2011) 3004–3021, https://doi.org/10.1039/c0cp01539c.

[45] J. Zhai, T.M. Hinton, L.J. Waddington, C. Fong, N. Tran, X. Mulet, C.J. Drummond, B.W. Muir, Lipid-PEG Conjugates Sterically Stabilize and Reduce the Toxicity of Phytantriol-Based Lyotropic Liquid Crystalline Nanoparticles, Langmuir. 31 (2015) 10871–10880, https://doi.org/10.1021/acs.langmuir.5b02797.

[46] A. Ganem-Quintanar, D. Quintanar-Guerrero, P. Buri, Monolein: A review of the pharmaceutical applications, Drug Dev. Ind. Pharm. 26 (2000) 809–820, https://doi.org/10.1081/DDC-100101304.

[47] T. Kojarunchitt, S. Hook, S. Rizwan, T. Rades, S. Baldursdottir, Development and characterisation of modified poloxamer 407 thermoresponsive depot systems containing cubosomes, Int. J. Pharm. 408 (2011) 20–26, https://doi.org/10.1016/j.ijpharm.2011.01.037.

[48] S.P. Akhlaghi, I.R. Ribeiro, B.J. Boyd, W. Loh, Impact of preparation method and variables on the internal structure, morphology, and presence of liposomes in phytantriol-Pluronic® F127 cubosomes, Colloids Surfaces B Biointerfaces. 145 (2016) 845–853, https://doi.org/10.1016/J.COLSURFB.2016.05.091.

[49] E.C. Rodrigues, M.A. Morales, S.N. De Medeiros, N.M. Suguihiro, E.M. Baggio-Saitovitch, Pluronic® coated sterically stabilized magnetite nanoparticles for

[50] N. Tran, M. Hocquet, B. Eon, P. Sangwan, J. Ratcliffe, T.M. Hinton, J. White, B. Ozcelik, N.P. Reynolds, B.W. Muir, Non-lamellar lyotropic liquid crystalline nanoparticles enhance the antibacterial effects of rifampicin against Staphylococcus aureus, J. Colloid Interface Sci. 519 (2018) 107–118, https://doi.org/10.1016/j.jcis.2018.02.048.

[51] C.H. Lee, Y.W. Chien, Drug Delivery: Vaginal Route, CRC Press, 2013. https://doi.org/10.1081/e-ept4-120050257.

[52] F.C. Carvalho, M.L. Bruschi, R.C. Evangelista, M.P.D. Gremião, Mucoadhesive drug delivery systems, Brazilian, J. Pharm. Sci. 46 (2010) 1–17, https://doi.org/10.1590/S1984-82502010000100002.

[53] S.M. Sagnella, C.E. Conn, I. Krodkiewska, X. Mulet, C.J. Drummond, Anandamide and analogous endocannabinoids: A lipid self-assembly study, Soft Matter. 7 (2011) 5319–5328, https://doi.org/10.1039/c1sm05141e.

[54] E. Esposito, R. Cortesi, M. Drechsler, L. Paccamiccio, P. Mariani, C. Contado, E. Stellin, E. Menegatti, F. Bonina, C. Puglia, Cubosome dispersions as delivery systems for percutaneous administration of indomethacin, Pharm. Res. 22 (2005) 2163–2173, https://doi.org/10.1007/s11095-005-8176-x.

[55] H. Wu, J. Li, Q. Zhang, X. Yan, L. Guo, X. Gao, M. Qiu, X. Jiang, R. Lai, H. Chen, A novel small Odorranalectin-bearing cubosomes: Preparation, brain delivery and pharmacodynamic study on amyloid-β25–35-treated rats following intranasal administration, Eur. J. Pharm. Biopharm. 80 (2012) 368–378, https://doi.org/10.1016/J.EJPB.2011.10.012.

[56] A. Saupe, K.C. Gordon, T. Rades, Structural investigations on nanoemulsions, solid lipid nanoparticles and nanostructured lipid carriers by cryo-field emission scanning electron microscopy and Raman spectroscopy, Int. J. Pharm. 314 (2006) 56–62, https://doi.org/10.1016/j.ijpharm.2006.01.022.

[57] M. Sato, P. da Silva, R. de Souza, K. dos Santos, M. Chorilli, Recent Advances in Nanoparticle Carriers for Coordination Complexes, Curr. Top. Med. Chem. 15 (2015) 287–297, https://doi.org/10.2174/1568026615666150108145614.

[58] S. Quignard, G. Frébourg, Y. Chen, J. Fattaccioli, Nanometric emulsions encapsulating solid particles as alternative carriers for intracellular delivery, Nanomedicine 11 (2016) 2059–2072, https://doi.org/10.2217/nnm-2016-0074.

[59] A.G. Cuenca, H. Jiang, S.N. Hochwald, M. Delano, W.G. Cance, S.R. Grobmyer, Emerging implications of nanotechnology on cancer diagnostics and therapeutics, Cancer 107 (2006) 459–466, https://doi.org/10.1002/cncr.22035.

[60] Y. Bai, H. Xing, P. Wu, X. Feng, K. Hwang, J.M. Lee, X.Y. Phang, Y. Lu, S.C. Zimmerman, Chemical Control over Cellular Uptake of Organic Nanoparticles by Fine Tuning Surface Functional Groups, ACS Nano. 9 (2015) 10227–10236, https://doi.org/10.1021/acsnano.5b03909.

[61] R.H. Müller, K. Mäder, S. Gohla, Solid lipid nanoparticles (SLN) for controlled drug delivery - a review of the state of the art, Eur. J. Pharm. Biopharm. 50 (2000) 161–177, https://doi.org/10.1016/S0939-6411(00)00087-4.

[62] J.D. Smart, The basics and underlying mechanisms of mucoadhesion, Adv. Drug Deliv. Rev. 57 (2005) 1556–1568, https://doi.org/10.1016/J.ADDR.2005.07.001.

[63] N. Hussain, Bioadhesive Drug Delivery Systems: Fundamentals, novel approaches and development, Int. J. Pharm. 205 (1-2) (2000) 201–202.

[64] J.D. Smart, R.G. Riley, J. Tsibouklis, S.A. Young, F.C. Hampson, J.A. Davis, G. Kelly, P.W. Dettmar, W.R. Wilber, The retention of 14C-labelled poly(acrylic acids) on gastric and oesophageal mucosa: an in vitro study, Eur. J. Pharm. Sci. 20 (2003) 83–90, https://doi.org/10.1016/S0928-0987(03)00175-1.

[65] R.M. Machado, A. Palmeira-de-Oliveira, C. Gaspar, J. Martinez-de-Oliveira, R. Palmeira-de-Oliveira, Studies and methodologies on vaginal drug permeation, Adv. Drug Deliv. Rev. 92 (2015) 14–26, https://doi.org/10.1016/j.addr.2015.02.003.

[66] C. Zihni, C. Mills, K. Matter, M.S. Balda, Desmosomes Tight junctions: from simple barriers to multifunctional molecular gates, Nat. Publ. Gr. 17 (9) (2016) 564–580.

[67] I. Leonida, D. Mihaela, Kumar, Springer Briefs in Bioengineering Bionanomaterials for Skin Regeneration, Springer International Publishing, 2016. http://www.springer.com/series/10280.

[68] B. Fonseca-Santos, B.V. Bonifácio, T.M. Baub, M.P.D. Gremião, M. Chorilli, In-situ gelling liquid crystal mucoadhesive vehicle for curcumin buccal administration and its potential application in the treatment of oral candidiasis, J. Biomed. Nanotechnol. 16 (2019) 1334–1344, https://doi.org/10.1166/jbn.2019.2758.

[69] L. Treuel, X. Jiang, G.U. Nienhaus, New views on cellular uptake and trafficking of manufactured nanoparticles, J. R. Soc. Interface. 10 (82) (2013) 20120939.

[70] J.D. Unciti-Broceta, V. Cano-Cortés, P. Altea-Manzano, S. Pernagallo, J.J. Díaz-Mochón, R.M. Sánchez-Martín, Number of nanoparticles per cell through a spectrophotometric method - A key parameter to assess nanoparticle-based cellular assays, Sci. Rep. 5 (2015) 1–10, https://doi.org/10.1038/srep10091.

[71] S. Ashraf, A. Hassan Said, R. Hartmann, M.A. Assmann, N. Feliu, P. Lenz, W.J. Parak, Quantitative Particle Uptake by Cells as Analyzed by Different Methods, Angew. Chemie - Int. Ed. 59 (2020) 5438–5453, https://doi.org/10.1002/anie.201906303.

[72] S. Kayacan, K. Yilancioglu, A. Seda Akdemir, F. Kaya Dagistanli, G. Melikoglu, M. Ozturk, The Effects of Apigenin and Curcumin on Autophagy Related Cell Death and Apoptosis, Proceedings. (2018) 1–4, https://doi.org/10.3390/proceedings2251586.

[73] F. Ahmadi, M. Ghasemi-Kasman, M. Gholamitabar Tabari, R. Pourbagher, S. Kazemi, A. Alinejad-Mir, Induction of apoptosis in hela cancer cells by an ultrasonic-mediated synthesis of curcumin-loaded chitosan-alginate-sTPP

nanoparticles, Int. J. Nanomed. (2017) 12–8545, https://doi.org/10.2147/IJN.S146516.

[74] B.P. Dyett, H. Yu, B. Lakic, N. De Silva, A. Dahdah, L. Bao, E.W. Blanch, C.J. Drummond, C.E. Conn, Delivery of antimicrobial peptides to model membranes by cubosome nanocarriers, J. Colloid Interface Sci. 600 (2021) 14–22, https://doi.org/10.1016/j.jcis.2021.03.161.

[75] A. Wieber, T. Selzer, J. Kreuter, Physico-chemical characterisation of cationic DOTAP liposomes as drug delivery system for a hydrophilic decapeptide before and after freeze-drying, Eur. J. Pharm. Biopharm. 80 (2012) 358–367, https://doi.org/10.1016/j.ejpb.2011.11.008.

[76] S. Lerch, M. Dass, A. Musyanovych, K. Landfester, V. Mailänder, Polymeric nanoparticles of different sizes overcome the cell membrane barrier, Eur. J. Pharm. Biopharm. 84 (2013) 265–274, https://doi.org/10.1016/j.ejpb.2013.01.024.

[77] L.-H. Tan, K.-G. Chan, P. Pusparajah, W.-L. Lee, L.-H. Chuah, T.M. Khan, L.-H. Lee, B.-H. Goh, Targeting Membrane Lipid a Potential Cancer Cure?, Front Pharmacol. 8 (2017), https://doi.org/10.3389/fphar.2017.00012.

[78] L.-H. Mu, L.-H. Wang, T.-F. Yu, Y.-N. Wang, H. Yan, P. Liu, C. Yan, V. Pallottini, Triterpenoid saponin ag8 from ardisia gigantifolia stapf Induces triple negative breast cancer cells apoptosis through oxidative stress pathway, Oxid. Med. Cell. Longev. 2020 (2020) 1–11.

[79] D. Ribatti, B. Nico, A. Vacca, L. Roncali, P.H. Burri, V. Djonov, Chorioallantoic membrane capillary bed: A useful target for studying angiogenesis and anti-angiogenesis in vivo, Anat. Rec. 264 (2001) 317–324, https://doi.org/10.1002/ar.10021.

[80] E.I. Deryugina, J.P. Quigley, Chapter 2 Chick Embryo Chorioallantoic Membrane Models to Quantify Angiogenesis Induced by Inflammatory and Tumor Cells or Purified Effector Molecules,, Methods Enzymol. 444 (2008) 21–41, https://doi.org/10.1016/S0076-6879(08)02802-4.

[81] P. Carmeliet, Angiogenesis in health and disease, Nat. Med. 9 (2003) 653–660, https://doi.org/10.1038/nm0603-653.

[82] A.E. Gururaj, M. Belakavadi, D.A. Venkatesh, D. Marmé, B.P. Salimath, Molecular mechanisms of anti-angiogenic effect of curcumin, Biochem. Biophys. Res. Commun. 297 (2002) 934–942, https://doi.org/10.1016/S0006-291X(02)02306-9.

[83] V.R. Yadav, S. Suresh, K. Devi, S. Yadav, Novel formulation of solid lipid microparticles of curcumin for anti-angiogenic and anti-inflammatory activity for optimization of therapy of inflammatory bowel disease, J. Pharm. Pharmacol. 61 (2009) 311–321, https://doi.org/10.1211/jpp/61.03.0005.

[84] F.D. Victorelli, V.M.d.O. Cardoso, N.N. Ferreira, G.M.F. Calixto, C.R. Fontana, F. Baltazar, M.P.D. Gremião, M. Chorilli, Chick embryo chorioallantoic membrane as a suitable in vivo model to evaluate drug delivery systems for cancer treatment: A review, Eur. J. Pharm. Biopharm. 153 (2020) 273–284.

[85] R. Swadi, G. Mather, B.L. Pizer, P.D. Losty, V. See, D. Moss, Optimising the chick chorioallantoic membrane xenograft model of neuroblastoma for drug delivery, BMC Cancer. 18 (2018) 1–11, https://doi.org/10.1186/s12885-017-3978-x.

[86] D. Ribatti, The chick embryo chorioallantoic membrane as a model for tumor biology, Exp. Cell Res. 328 (2014) 314–324, https://doi.org/10.1016/J.YEXCR.2014.06.010.

[87] D. Mandracchia, G. Tripodo, A. Trapani, S. Ruggieri, T. Annese, T. Chlapanidas, G. Trapani, D. Ribatti, Inulin based micelles loaded with curcumin or celecoxib with effective anti-angiogenic activity, Eur. J. Pharm. Sci. 93 (2016) 141–146, https://doi.org/10.1016/j.ejps.2016.08.027.

[88] V. Sethuraman, K. Janakiraman, V. Krishnaswami, S. Natesan, R. Kandasamy, pH responsive delivery of lumefantrine with calcium phosphate nanoparticles loaded lipidic cubosomes for the site specific treatment of lung cancer, Chem. Phys. Lipids. 224 (2019), https://doi.org/10.1016/j.chemphyslip.2019.03.016 104763.

[89] M. Liu, S. Xie, J. Zhou, Use of animal models for the imaging and quantification of angiogenesis, Exp. Anim. 67 (1) (2018) 1–6.

[90] H. Lv, S. Zhang, B. Wang, S. Cui, J. Yan, Toxicity of cationic lipids and cationic polymers in gene delivery, J. Control. Release. 114 (2006) 100–109, https://doi.org/10.1016/j MailCleaner quarantine report.jconrel.2006.04.014.

[91] X. Peng, Y. Zhou, K. Han, L. Qin, L. Dian, G. Li, X. Pan, C. Wu, Characterization of cubosomes as a targeted and sustained transdermal delivery system for capsaicin, Drug Des. Devel. Ther. 9 (2015) 4209–4218, https://doi.org/10.2147/DDDT.S86370.

[92] L. Boge, K. Hallstensson, L. Ringstad, J. Johansson, T. Andersson, M. Davoudi, P. T. Larsson, M. Mahlapuu, J. Håkansson, M. Andersson, Cubosomes for topical delivery of the antimicrobial peptide LL-37, Eur. J. Pharm. Biopharm. 134 (2019) 60–67, https://doi.org/10.1016/j.ejpb.2018.11.009.